Side-lobe Suppression and Beam Collimation in the Generation of Vortex Electromagnetic Waves for Radar Imaging

Yuliang Qin, Kang Liu, Yongqiang Cheng, Xiang Li, Hongqiang Wang, and Yue Gao

***Abstract*—For the electromagnetic (EM) vortex imaging purposes, the side-lobe suppression and the beam collimation method in the generation of OAM-beams is proposed. Based on the concentric-ring array, the objective function for the generic algorithm (GA) is defined to calculate the signal amplitude for each ring. Comprehensive simulations are conducted to validate the effectiveness of the proposed method. Results show that the main lobes of the radiation pattern of different OAM modes are collimated in the same direction and the side lobes are all lower than -20 dB. Furthermore, the imaging model of the concentric-ring array is established and the target image is obtained through numerical simulations. The work can advance the development of the EM vortex imaging technique and novel radar detection technology as well.**

***Index Terms*—Orbital angular momentum, radar imaging, radiation pattern optimization, vortex electromagnetic wave**

I. Introduction

In recent years, there has been a growing interest in the orbital angular momentum (OAM), which is carried by the vortex electromagnetic (EM) wave possessing helical phase fronts [1]. Compared with traditional waves, the phase front of the vortex EM wave has an azimuthally dependent phase factor $\exp(il\phi)$. Hence, the Poynting vector for each point within the beam is perpendicular to the phase front and has an azimuthal momentum component [2].

Since the year of 2007, the OAM has been applied in the radio domain, which might offer a solution to the problem of radio-band congestion [1], [3], [4]. However, OAM multiplexing in the wireless communication has also caused controversy [5]. For radar detection and imaging realms, the helical phase-front can be exploited to improve the resolution of the cross-range profile of the target [6]-[8]. In [7], [9], the concentric uniform circular arrays are designed to adjust the main-lobe directions of the OAM beams with different modes. However, the side lobes of the pattern are still high, which may lead to negative influences on the radar detection and imaging applications.

In this letter, for the EM vortex imaging purposes, the radiation pattern optimization method is proposed to collimate the beams for different OAM modes and suppress the side lobes simultaneously. Firstly, the concentric-ring array is presented and the radiation pattern is derived. Secondly, the fitness function of the genetic algorithm (GA) is defined to calculate the amplitude of the excitation signal for each ring. Finally, the imaging model based on the concentric uniform circular arrays is derived and the target image is obtained by numerical simulations.

II. Side-lobe Suppression and Beam Collimation Method

Hitherto, the uniform circular array (UCA) has been widely used in the generation of OAM beams, for example, the OAM-based wireless communication [3] and the electromagnetic vortex imaging [6]. However, the side lobes of the radiation pattern are much high and the inconsistency of the main-lobe directions of beams carrying different OAM modes needs to be eliminated [7]. Therefore, the concentric UCAs (Fig. 1) are applied to suppress the side lobes and collimate the beams with different modes simultaneously.

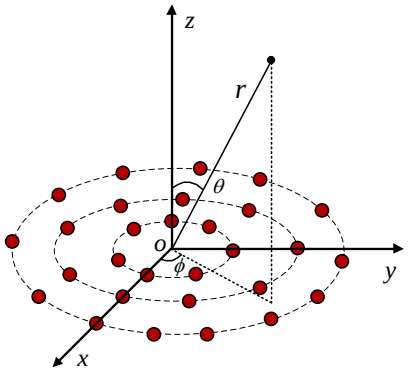

Fig. 1. The sketch map of the array configuration.

Here, the incrementally phased method [3] is applied to generate the vortex EM wave and the total radiation pattern $F(\theta,\phi)$ of the array can be given by

Y. Qin, K. Liu, Y. Cheng, X. Li, and H. Wang are with the College of Electronic Science and Engineering, National University of Defense Technology, Changsha 410073, China (e-mail: liukang1117@126.com).

K. Liu and Y. Gao are also with the School of Electronic Engineering and Computer Science, Queen Mary University of London, London E1 4NS, UK.

This work was supported by the National Natural Science Foundation of China under Grant No. 61302149 and by the National Natural Science Foundation of China under Grant No. 61571011.

$$F(\theta,\phi)=\left|\sum_{h=1}^{H}\sum_{n=1}^{N_h} f(\theta,\phi-\phi_{hn})I_h\exp\{ika_h\sin\theta\cos(\phi-\phi_{hn})\}\cdot\exp(il\phi_{hn})\right|$$
$$\approx f(\theta,\phi)\sum_{h=1}^{H} I_h J_l(ka_h\sin\theta)$$
$$\triangleq f(\theta,\phi)\cdot AF(\theta,\phi) \quad (1)$$

where H denotes the number of rings, a_h is the radius of the h^{th} ring and I_h is the amplitude of the excitation signal. $N_h=[4\pi a_h/\lambda]$ is the number of the array antennas of the h^{th} ring. l denotes the OAM mode number (also called "topological charge"), ϕ_{hn} is the azimuthal angle of the array element, and $f(\theta,\phi-\phi_{hn})$ denotes the directional pattern of the antenna. $AF(\theta,\phi)=\sum_{h=1}^{H} I_h J_l(ka_h\sin\theta)$ indicates the array factor and $k=2\pi f/c$ is the wave number, where f is the frequency and c denotes the light speed in the vacuum. In this letter, we assume that each element has the same pattern

$$f(\theta,\phi)=\frac{1+\cos(\pi\sin\theta)}{\cos\theta} \quad (2)$$

where $-\pi/2\le\theta\le\pi/2$ and $0\le\phi\le2\pi$.

Now, the generic algorithm is exploited to design the excitation coefficient for each ring. Based on the GA principle, the fitness function is defined as

$$fitness=w_1\frac{|\theta_0-\theta_{\text{des}}|}{180^\circ}+w_2|SLL_{\max}-SLL_{\text{des}}| \quad (3)$$

where $SLL_{\max}$ and SLL_{des} denote the calculated and the designed highest side-lobe levels, respectively. w_1 and w_2 are the weighting coefficients, which are usually decided by the expected characteristics of the designed pattern. θ_0 signifies the calculated position of the main lobe and θ_{des} is the expected direction of the main lobe, which can be obtained by means of a linear fit method [9]

$$\theta_{\text{des}}=\arcsin[(1.0509l_{\max}+1.1562)/(ka_{\max})] \quad (4)$$

where $l_{\max}$ denotes the largest OAM mode number exploited in the electromagnetic vortex imaging and $a_{\max}$ is radius of the outer ring.

According to Eqs. (3) and (4), numerical methods are applied to calculate the amplitude of the excitation signal for each ring. In the simulations, the key parameters are $f=10$ GHz, $l_{\max}=10$ and $a_{\max}=10\lambda$, where λ is the signal wavelength. The spacing on the arc between two array elements is $\lambda/2$ and the number of rings is $H=10$. Based on Eq. (4), the expected main-lobe direction is $\theta_{des}=10.69^\circ\approx11^\circ$. The calculated feed coefficients for each ring are shown in Table 1. It can be seen from the results that the signal amplitude for each ring are usually different for different OAM modes. For large OAM modes, more rings are applied to optimize the radiation pattern.

TABLE I
THE FEED COEFFICIENTS FOR EACH RING

Radius	l=1	l=2	l=3	l=4	l=5	l=6	l=7	l=8	l=9	l=10
$a_1=\lambda$	1	0.71	0.79	0.54	0	0.48	0	0	0	0
$a_2=2\lambda$	0.95	1	0.75	0.42	0.48	0.53	0.43	0.93	0.77	0.31
$a_3=3\lambda$	0	0.87	1	0.97	0.39	0.29	0.12	0.15	0.72	0.31
$a_4=4\lambda$	0	0	0.64	1	0.98	0.55	0.32	0	0	0
$a_5=5\lambda$	0	0	0	0.78	1	0.98	0.46	0.38	0.29	0
$a_6=6\lambda$	0	0	0	0	0.78	1	0.98	0.89	0.20	0.23
$a_7=7\lambda$	0	0	0	0	0	0.76	1	0.80	0.77	0.67
$a_8=8\lambda$	0	0	0	0	0	0	0.75	1	0.85	0.97
$a_9=9\lambda$	0	0	0	0	0	0	0	0.60	1	0.98
$a_{10}=10\lambda$	0	0	0	0	0	0	0	0	0.48	1

The designed radiation patterns for different OAM modes are depicted in Fig. 2 and the corresponding phase-front distributions are shown in Fig. 3. The blue dotted line in Fig. 2 signifies the traditional results when all the elements are fed uniformly, while the red solid line depicts the optimized pattern based on the GA method. It is clear from Fig. 2 and Table 2 that all the main lobes of different OAM modes are nearly directed at the same elevation angle and the side-lobe level is suppressed effectively (lower than -20 dB), which can meet the demand of the EM vortex imaging. As shown in Fig. 3, the beams are sampled at a distance $z=100$ m from the transmitting array and the sample window is 10 m wide in both x- and y-directions. The change in color from blue to red and back to blue again corresponds to a change in phase of 2π. The phase-front distribution has a regular helical shape, which means the generated beams still keep the key characteristic of the vortex EM wave [1].

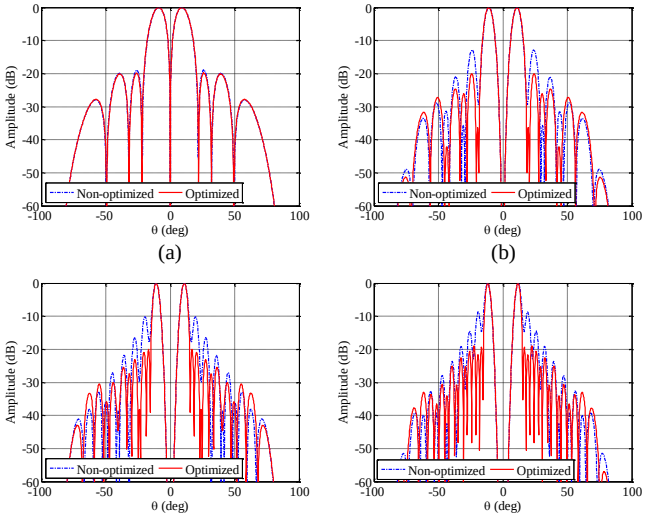

Fig. 2. The radiation pattern as a function of the elevation angle θ ($\phi=0^\circ$). (a) l=1, (b) l=4, (c) l=7, (d) l=10.

TABLE II
THE DIRECTION OF THE MAIN LOBE

Topological charge	Direction of the main lobe /°	Main-lobe Width /°
l=1	8.8	10.2
l=2	10.2	8
l=3	11	7
l=4	11	6
l=5	11	5.2
l=6	11	4.6
l=7	11	4.2
l=8	11	4

l=9	11	3.6
l=10	11.6	3.6

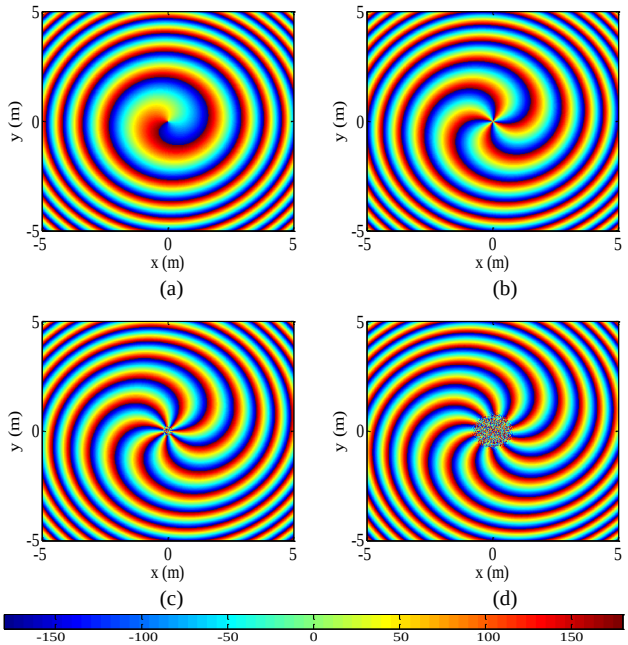

Fig. 3. Phase front distribution. (a) l=1, (b) l=4, (c) l=7, (d) l=10.

III. Electromagnetic Vortex Imaging Based on the Concentric-ring Array

In the previous section, the radiation pattern of the OAM beam is optimized using the concentric-ring array, which is helpful to the clutter suppression for radar imaging. Here, the EM vortex imaging model is derived and the imaging results are analyzed based on the suppressed and collimated OAM beams.

For the concentric-ring array designed in Section II, the emitted signal $S(\boldsymbol{r},l)$ can written as follows:

$$S(\boldsymbol{r},l)=\frac{e^{-ikr}}{r}i^l e^{il\phi}\sum_{h=1}^{H}I_h J_l(ka_h\sin\theta) \tag{5}$$

To reduce the system complexity, a single antenna at the origin is exploited to receive the echo and the echo $S_r(\boldsymbol{r},l)$ can be expressed as:

$$S_r(\boldsymbol{r},l)=\sum_{m=1}^{M}\sigma_m\frac{e^{-i2kr_m}}{r_m^2}i^l e^{il\phi_m}\sum_{h=1}^{H}I_h J_l(ka_h\sin\theta_m) \tag{6}$$

where M denotes the number of scattering points, (r_m,θ_m,ϕ_m) is the position of the m^{th} scattering point, and σ_m signifies the radar cross section (RCS).

Then, the normalized echo is

$$S_r(\boldsymbol{r},l)=\sum_{m=1}^{M}\sigma_m e^{-i2kr_m}e^{il\phi_m}\sum_{h=1}^{H}I_h J_l(ka_h\sin\theta_m) \tag{7}$$

Based on Eq. (7), we can find that the OAM mode number and the variable of the azimuthal angle keep an approximate dual relationship. Therefore, the 2-D FFT can be performed to obtain the target image in the range-azimuth domain.

In the simulations, a plane model is assumed to be the target, the center frequency is $f_0=10\,\text{GHz}$, and the bandwidth is $B=500\,\text{MHz}$. The array configuration is the same as that designed in the previous section and the OAM mode number exploited to image the target is $l\in[-10,10]$. It is clear from Fig. 4(a) ad Fig. 4(b) that the Taylor window can be applied to effectively suppress the side lobes. However, the main lobe will widen, which leads to a decline of the imaging resolution. Moreover, the influence of the noise on the imaging quality is numerically simulated. In the simulations, the Gaussian white noise is added to the echo and the signal to noise ratio is set as $SNR=5\,\text{dB}$. Results in Fig. 4(c) and Fig. 4(d) demonstrate that the proposed imaging method is much robust against the noise.

In general, compared with non-optimized OAM beams, the suppressed and collimated OAM beams can guarantee the main lobes of different OAM beams illustrate the same area where the target may exist. Moreover, the suppressed and collimated beams is beneficial to improve the signal-to-noise ratio in the real application scenario and suppress the background clutter for radar imaging.

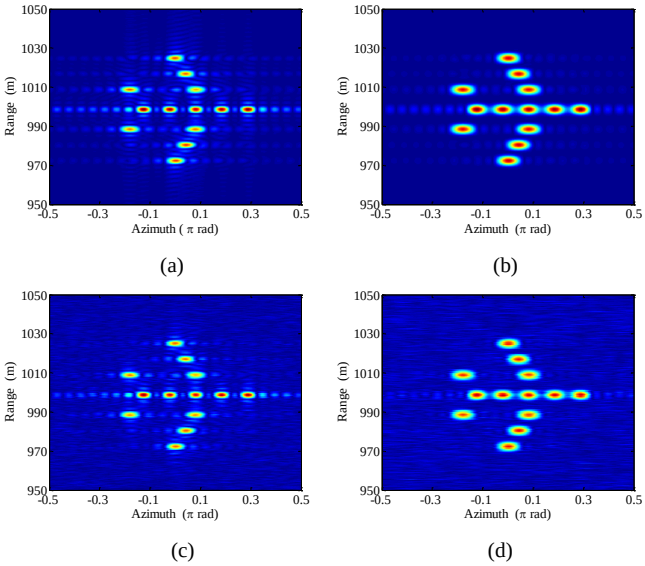

Fig. 4. Imaging results using the concentric-ring array. (a) Imaging results without window or noise contribution, (b) Imaging results with window contribution (no noise), (c) Imaging results with noise contribution (no window), (d) Imaging results with window and noise contributions.

IV. Conclusion

To conclude, the pattern synthesis method is proposed to suppress the side lobes and collimate the beams in the generation of vortex electromagnetic waves. Moreover, the imaging model is established based on the concentric-ring array and the plane model is imaged. Results demonstrate that the concentric-ring array can be readily exploited to generate OAM beams and image the targets, which is robust against the noise. The work and results can benefit the development of OAM-based radar system, e.g., its applications in the scenario where the clutter exists.

References

[1] B. Thidé et al., "Utilization of photon orbital angular momentum in the low-frequency radio domain," *Phys. Rev. Lett.*, vol. 99, no. 8, p. 087701, 2007.

[2] L. Allen et al., “Orbital angular momentum of light and the transformation of Laguerre-Gaussian laser modes,” *Phys. Rev. A*, vol. 45, no. 11, pp. 8185–8189, Jun. 1992.
[3] S. M. Mohammadi et al., “Orbital angular momentum in radio- a system study,” *IEEE Trans. Antenn. Propag.*, vol. 58, no. 2, pp. 565–572, Feb. 2010.
[4] F. Tamburini, E. Mari, A. Sponselli, B. Thidé, A. Bianchini, and F. Romanato, “Encoding many channels on the same frequency through radio vorticity: First experimental test,” *New J. Phys.*, vol. 14, no. 3, p. 033001, Mar. 2012.
[5] K. Liu et al., “Generation of OAM Beams Using Phased Array in the Microwave Band,” *IEEE Trans. Antenn. Propag.*, vol. 64 no. 9, pp. 3850–3857, Sep. 2016.
[6] K. Liu, Y. Cheng, Z. Yang, H. Wang, Y. Qin, and X. Li, “Orbital-angular-momentum-based electromagnetic vortex imaging,” *IEEE Antennas Wireless Propag. Lett.*, vol. 14, pp. 711–714, 2015.
[7] K. Liu et al., “Generation of Orbital Angular Momentum Beams for Electromagnetic Vortex Imaging,” *IEEE Antennas and Wireless Propagation Letters*, DOI: 10.1109/LAWP.2016.2542187, 2016.
[8] M.T. Lin et al., “Super-resolution orbital angular momentum based radar targets detection,” *IET Electronics Letters*, vol. 52, no. 13, pp. 1168-1170, 2016.
[9] T.Z. Yuan et al., “Electromagnetic Vortex Imaging Using Uniform Concentric Circular Arrays,” *IEEE Antennas and Wireless Propagation Letters*, vol. 15, pp. 1024-1027, 2016.